3B

MICHIGAN STATE
UNIVERSITY

National Superconducting Cyclotron Laboratory

β-DECAY PROPERTIES OF ^{55,56}Ti

**P.F. MANTICA, B.A. BROWN, A.D. DAVIES,
T. GLASMACHER, D.E. GROH, M. HOROI,
S.N. LIDDICK, D.J. MORRISSEY, A.C. MORTON,
W.F. MUELLER, H. SCHATZ, A. STOLZ, and S.L. TABOR**

NSCL

MSUCL-1272 **AUGUST 2003**

β-decay properties of ^{55,56}Ti

P.F. Mantica[1,2], B.A. Brown[1,3], A.D. Davies[1,3], T. Glasmacher[1,3],
D.E. Groh[1,2], M. Horoi[4], S.N. Liddick[1,2], D.J. Morrissey[1,2],
A.C. Morton[1], W.F. Mueller[1], H. Schatz[1,3], A. Stolz[1], and S.L. Tabor[5]

(1) *National Superconducting Cyclotron Laboratory, Michigan State University, East Lansing, Michigan 48824*

(2) *Department of Chemistry, Michigan State University, East Lansing, Michigan 48824*

(3) *Department of Physics and Astronomy, Michigan State University, East Lansing, Michigan 48824*

(4) *Department of Physics, Central Michigan University, Mount Pleasant, Michigan 48859 and*

(5) *Department of Physics, Florida State University, Tallahassee, Florida 32306*

(Dated: August 7, 2003)

Abstract

β decay of the neutron-rich nuclides ^{55,56}Ti has been used to populate low-energy levels of ^{55,56}V, respectively. A half-life of 1.3 ± 0.1 s was deduced for ^{55}Ti, significantly longer than that determined from previous measurements. The β decay of ^{56}Ti is characterized by a short half-life of 200 ± 5 ms, with nearly all of the decay directly populating the 1^+ ground state of ^{56}V. The role of the spin-flip process $\nu f_{5/2} \rightarrow \pi f_{7/2}$ in defining the β-decay properties of nuclei near $N = 32$, including ^{55,56}Ti, is discussed.

INTRODUCTION

The energy level systematics of the even-even $_{20}$Ca, $_{22}$Ti, and $_{24}$Cr nuclides have revealed a substantial subshell closure at $N = 32$, corresponding to the filling of the $\nu p_{3/2}$ single-particle orbital [1–4]. The presence of this spherical subshell gap is the result of a diminished $\nu f_{5/2}$ - $\pi f_{7/2}$ monopole interaction as protons are removed from the $f_{7/2}$ orbital. In general, the strongly attractive (proton $j = \ell + 1/2$) - (neutron $j = \ell - 1/2$) monopole term in the nucleon-nucleon interaction should play an important role in defining the magic numbers in exotic nuclei [5]. Furthermore, the spin-orbit coupling partners help define the β-decay properties of exotic nuclei. As an example, the β-decay half-lives of neutron-rich $\pi f_{7/2}$ nuclides with $N = 33$ are markedly shorter that those of their $N = 32$ counterparts. The next available neutron orbital above $N = 32$ is expected to be $\nu f_{5/2}$, the spin-orbit partner of the occupied proton orbital $\pi f_{7/2}$.

Table I includes the measured half-lives for $N = 32$ and $N = 33$ nuclides from $_{19}$K to $_{25}$Mn, where the data are taken from Refs. [2, 6–9]. The K nuclides with $N = 32$ and $N = 33$ are expected to have a single hole in the proton *sd* shell, therefore, a fast $\nu f_{5/2} \rightarrow \pi f_{7/2}$ spin-flip transition would not be expected with a crossing of the $N = 32$ subshell closure. Indeed, a difference of only a factor of 3 is observed between the β-decay half-lives of the K isotopes with $N = 32$ and those with $N = 33$. Starting at $Z = 20$, the proton *sd* shell is filled, and the next available proton orbital is $1f_{7/2}$. For the elements $_{20}$Ca to $_{25}$Mn, there is at least one order-of-magnitude difference between the half-lives of the $N = 32$ and $N = 33$ isotopes, except for $_{22}$Ti. The greatest difference between the $N = 32$ and $N = 33$ half-lives is observed for Ca, where the short half-life of ^{53}Ca [10] has been attributed by Sorlin *et al.* [7] to the spin-flip process $\nu f_{5/2} \rightarrow \pi f_{7/2}$.

We report new results for the β-decay properties of the neutron-rich ^{55,56}Ti isotopes. A first study of the β-decay properties of ^{55,56}Ti was completed by Dörfler *et al.* [8] and included the measurement of β-delayed γ rays using a highly-efficient, but low resolution BGO array. β-decay half-lives for ^{55,56}Ti have also been measured by Ameil *et al.* [9], and their results suggested a faster β decay for the $N = 33$ isotone ^{55}Ti: $T_{1/2} = 320 \pm 60$ ms compared to $T_{1/2} = 600 \pm 40$ ms as measured by Dörfler *et al.* The faster decay rate reported by Ameil *et al.* is in better agreement with the observed decay rates for other $N = 33$ isotones, which may indicate a spin-flip $\nu f_{5/2} \rightarrow \pi f_{7/2}$ decay. The goals of the current β-decay studies were to resolve the discrepancy in the half-life of $^{55}Ti_{33}$ and to measure β-delayed γ rays using a high-resolution Ge array to deduce the low-energy level structure of the daughter $^{55,56}V$ nuclides.

EXPERIMENTAL TECHNIQUE

The $^{55,56}Ti$ parent nuclides were produced using the experimental facilities at the National Superconducting Cyclotron Laboratory (NSCL) at Michigan State University as part of a larger study of the β-decay properties of neutron-rich nuclides near the $N = 32$ subshell closure. Results have previously been published for the neutron-rich isotopes $^{56-58}V$ [2] and ^{54}Sc [3]. A summary of the experimental techniques employed follows, while a detailed account of these techniques is available in the previous publications.

A 140-MeV/nucleon $^{86}Kr^{34+}$ beam was produced at an average beam current of 3 pnA using the coupled cyclotrons at the NSCL. The ^{86}Kr beam was fragmented in a 376-mg/cm^2 thick Be target located at the object position of the A1900 fragment separator [11]. The secondary fragments of interest were selected in the A1900 using a 330 mg/cm^2 Al degrader and 1% momentum slits; both were located at the intermediate image of the device. The fully-stripped fragments were implanted in a 985-μm thick double-sided Si microstrip detector (DSSD) that is part of the NSCL β counting system [12]. Fragments were unambiguously identified by a combination of multiple energy loss signals and time of flight. The desired Ti fragments were produced at two different values of the A1900 magnetic rigidities. A total of 3.3×10^5 ^{55}Ti implants were collected with the A1900 set to $B\rho_1 = 4.0417$ Tm and $B\rho_2 = 3.7554$ Tm, and 7.3×10^4 ^{56}Ti implants with $B\rho_1 = 4.1261$ Tm and $B\rho_2 = 3.8417$ Tm.

Fragment-β correlations were established in software by requiring a high-energy implant event in a single pixel of the DSSD followed by a low-energy β event in the same pixel. The differences between the absolute time stamps of correlated β and implant events were histogrammed to generate a decay curve. To suppress background, implants were rejected if they were not followed by a β event within ten seconds in the same pixel or if they were followed by a second implantation within ten seconds, also within the same pixel. The measured fragment-β correlation efficiencies were 30% and 40% for the A1900 magnetic rigidity settings leading to production of ^{55}Ti and ^{56}Ti, respectively.

Delayed γ rays were measured using six Ge detectors from the MSU Segmented Germanium Array (SeGA) [13] arranged around the β counting system. The energy resolution for each of the Ge detectors was measured to be $\sim$ 3.5 keV for the 1.3 MeV γ-ray transition in ^{60}Co. The peak efficiency for γ-ray detection with this array was 3.3% at 1 MeV.

RESULTS

^{55}Ti

The β-delayed γ-ray spectrum for ^{55}Ti in the range 0 to 2 MeV , shown in Fig. 1, contains $\beta\gamma$ events that occurred within the first second after a ^{55}Ti implant. Nine transitions have been assigned to the β decay of ^{55}Ti, and are listed in Table II. The peak at 518 keV in Fig. 1 corresponds to a transition in the daughter ^{55}V decay. The peak at 846 keV is assigned to long-lived ^{56}Mn ($T_{1/2} = 2.56$ h), which is the grand-daughter of ^{56}V, the primary component of the secondary beam. The intense transitions at 323 and 673 keV are most likely the transitions observed at 300 ± 100 keV and 700 ± 100 keV in the low resolution study by Dörfler *et al.* [8].

The decay curve derived from ^{55}Ti-correlated β decays is shown in Fig. 2(a). The curve was fitted with a single exponential decay with an exponential background component. The decay constant for the exponential background of 0.144 s^{-1} was deduced by fitting the decay curves for all nuclides implanted along with ^{55}Ti in the first A1900 tune as described in Ref. [2]. The activity of the daughter ^{55}V decay, with $T_{1/2} = 6.5$ s, was investigated and not found to contribute significantly to the decay curve. Decay curves were also obtained from $\beta\gamma$ coincidence data. The decay curves for β particles in coincidence with the 323- and 673-keV γ rays are also shown in Fig. 2. We have adopted a value of 1.3 ± 0.1 s for the half-life of ^{55}Ti. This half-life does not agree with results of previous half-life measurements for ^{55}Ti, 600 ± 40 ms [8] and 320 ± 60 ms [9], listed in Table I.

The proposed decay scheme for levels in ^{55}V populated following the β decay of ^{55}Ti is shown in Fig. 3. The β-decay Q value was derived from the measured mass excess of both parent and daughter as compiled in Ref. [14]. Absolute γ-ray intensities were deduced from the number of observed ^{55}Ti γ rays, the simulated γ-ray efficiency curve [2], and the number of ^{55}Ti implants correlated with β decays. The last term was derived from the fit of the decay curve in Fig. 2(a). Placement of the 828- and 1480-keV γ rays feeding the 673-keV state in

^{55}V was confirmed by $\gamma\gamma$ coincidences (see Fig. 4). The 652- and 1803-keV transitions were placed in the low-energy level scheme based on energy-sum relationships. No evidence for a 323-673 coincidence, suggested in Ref. [8], was found in our $\gamma\gamma$ correlation matrix.

β feedings to levels in ^{55}V were deduced from the absolute γ-ray intensities, and are summarized in Table III. The log*ft* values were interpolated using the tabulation in Ref. [15]. The $24 \pm 5\%$ branching ratio to the ^{55}V ground state is smaller than the $60 \pm 10\%$ branching ratio deduced by Dörfler *et al.* [8]. The observed β branches all have log*ft* values between 4 and 6, suggesting the transitions are allowed. The log*ft* values should be considered lower limits based on the sizeable β-decay Q-value window and the possible existence of unobserved decays. A ground-state spin and parity of $3/2^-$ was adopted by Dörfler *et al.* [8] for ^{55}Ti based on J^π systematics of the odd-A $N = 33$ isotones. One would expect $7/2^-$ spin-parity for the ground state of the ^{55}V daughter, and Nathan *et al.* [16] have suggested $3/2^- \leq J^\pi \leq 7/2^-$ based on characteristics of the β decay of the ^{55}V ground state to levels in ^{55}Cr.

^{56}Ti

The decay curve derived from ^{56}Ti-correlated β decays is shown in Fig. 5(a). The curve was fitted with a single exponential decay and exponential growth and decay of the short-lived daughter ^{56}V, whose half-life was taken as 216 ± 4 ms [2]. An exponential background with a decay constant 0.0815 s^{-1} [2] was also included in the fit. We have deduced a value of 200 ± 5 ms for the half-life of ^{56}Ti. This half-life is in good agreement with the results of previous half-life measurements for ^{56}Ti, 150 ± 30 ms [8] and 190 ± 40 ms [9].

The β-delayed γ-ray spectrum for the decay of ^{56}Ti in the range 0 to 1.5 MeV is shown in Fig. 5(b). The two prominent transitions at 668 and 1006 keV correspond to γ rays in ^{56}Cr emitted following decay of the daughter ^{56}V [2]. No evidence was found for ^{56}Ti delayed γ rays with absolute intensity greater than 2%. The "peak" appearing at 162 keV with 13 counts in only a single channel (see Fig. 5(b) inset) was considered to be a spectrum artifact. The absence of β-delayed γ rays following the decay of ^{56}Ti is in contrast to the findings of Dörfler *et al.* [8], who reported unresolved γ-ray intensity in the range 0.2 to 0.8 MeV accounting for 40% of the overall β feeding. The data reported here suggest little β branching to excited states in ^{56}V.

The absolute intensities of the 668- and 1006-keV γ rays were deduced to be $20 \pm 3\%$ and $24 \pm 4\%$, respectively, using the extracted peak areas, the simulated γ-ray efficiency curve [2], and the number of ^{56}Ti implants correlated with β decays. The γ-ray intensities deduced here, where ^{56}V was produced as a daughter radioactivity, compared to those from a study of the direct production and decay of ^{56}V [2], were found to be systematically low by $6 \pm 3\%$. One explanation that could account for the missing intensity is the presence of a β-delayed neutron branch following the decay of ^{56}Ti. A delayed-neutron branch is plausible; the β-decay Q value for ^{56}Ti is 7.1 ± 0.4 MeV [14], while the one-neutron separation energy in ^{56}V is 5.16 ± 0.26 MeV. We found no evidence for the known γ-ray transitions in ^{55}V [2] in Fig. 5(b) that would also be suggestive of a delayed neutron branch, however, this would require that such delayed neutron emission populates excited states in ^{55}V.

The deduced β branching to the daughter ^{56}V ground state is $94 \pm 3\%$ if all the missing γ-ray intensity following the decay of ^{56}V discussed above is attributed to a β-delayed neutron branch for the ^{56}Ti decay. This does not take into account possible unobserved transitions with intensities less than 2% that are likely present due to the large Q value for the ^{56}Ti β decay. The log*ft* value of 3.95 ± 0.12 determined for direct ground-state β branch suggests an allowed transition and is consistent with the 1^+ spin and parity assignment proposed for the ground state of ^{56}V [2, 7].

DISCUSSION

The half-life of ^{55}Ti reported here is significantly longer than that measured in Refs. [8, 9]. An incorrect particle identification of ^{55}Ti is unlikely as other isotopes in the beam cocktail were correctly correlated with both delayed and isomeric (^{54}Sc^m) γ rays. The delayed γ rays assigned to ^{55}Ti β decay in this work were also observed by Dörfler *et al.* [8]. However, the half-life determined for ^{55}Ti in Ref. [8] based on $\beta\gamma$ coincidences was 0.58 ± 0.05 s, about a factor of two shorter than the present value of 1.3 ± 0.1 s. Furthermore, our new result for the ^{55}Ti half-life and that of Dörfler *et al.* both disagree with the value of 0.32 ± 0.06 s obtained by Ameil *et al.* [9]. On the other hand, the half-life of ^{56}Ti was also measured in each of the three experiments, and reasonable agreement was realized between our measured half-life value of 200 ± 5 ms and those of Dörfler *et al.* (150 ± 30 ms) and Ameil *et al.* (190 ± 40 ms).

It is possible that a β-decaying isomer in ^{55}Ti has been populated, since all three experiments utilized different beam-target combinations. Such an isomer would not be resolved in the fragment particle identification spectrum. One method to differentiate possible isomeric states would be detailed γ-ray spectroscopy, since the presence of the isomer would suggest very different spin values for the β-decaying states and therefore different branchings to states in the daughter. We did not observe a statistically significant difference in the half-life values deduced from $\beta\gamma$ coincidences with individual gates on the 323-, 673-, and 1330-keV transitions.

The half-life value adopted here for $^{55}Ti_{33}$, 1.3$\pm$0.1 s, is nearly identical to that previously measured for $^{54}Ti_{32}$ [8], 1.5 $\pm$ 0.4 s. The rapid decrease in half-life values observed for Ca and other $\pi f_{7/2}$ isotopes across $N = 32$ (Table I) is not reproduced in the Ti isotopes.

Sorlin *et al.* attributed the short half-life of $^{53}Ca_{33}$ to the spin-flip process $\nu f_{5/2} \rightarrow \pi f_{7/2}$ [7]. However, transfer data for ^{49}Ca suggest that the $\nu p_{1/2}$ single-particle strength is about 1.8 MeV lower in energy than that for $\nu f_{5/2}$, all relative to the $\nu p_{3/2}$ ground state [17]. The re-ordering of the $\nu f_{5/2}$ and $\nu p_{1/2}$ single-particle orbitals, along with the large spin-orbit splitting between the $\nu p_{3/2}$ and $\nu p_{1/2}$ orbitals, is believed to be responsible for the appearance of a subshell gap at $N = 32$ [1] and a potential shell gap at $N = 34$ [5]. In addition, the decay of ^{53}Ca, with $Q_\beta = 10.0 \pm 0.6$ MeV [14], is observed to populate states in ^{53}Sc that are above the one-neutron separation energy [10] estimated to be 5.7 ± 0.4 MeV [14].

An alternative explanation for the fast β decay of $^{53}Ca_{33}$ (compared with that of $^{52}Ca_{32}$) is a $\nu p_{1/2}$ to $\pi p_{3/2}$ spin-flip decay, where the excited states in the daughter $^{53}Sc_{32}$ that have significant $\pi p_{3/2}$ components in the state wavefunction lie above the neutron separation energy. This scenario can account for both the fast decay and the large delayed-neutron branching observed for ^{53}Ca.

The nucleus $^{55}Ti_{33}$ differs from $^{53}Ca_{33}$ by the addition of two protons, presumably in the $\pi f_{7/2}$ orbital. As noted earlier, the half-life values of the Ti isotopes do not show a precipitous drop across $N = 32$. To better understand the near constancy of the half-lives for the Ti isotopes across $N = 32$, we have performed shell model calculations using the new pf-shell interaction GXPF1 [18] in the full pf-shell model space using the codes OXBASH [19] and CMICHSM [20].

The ground state of ^{55}Ti was calculated to have spin 1/2, and a doublet of states with spins 3/2 and 5/2 lies approximately 1 MeV above the ground state. The β-decay branching from the calculated $1/2^-$ ground state of ^{55}Ti to levels in ^{55}V below 2 MeV is shown in Fig. 6. The experimentally observed energy levels in ^{55}V are also shown in Fig. 6 for direct comparison with the shell model results. Without specific knowledge of the spins and parities of the ^{55}Ti parent and daughter states in ^{55}V, it is difficult to make detailed quantitative comparisons between experiment and theory. However, some qualitative distinctions can be made.

The relative positions of the $\nu p_{1/2}$ and $\nu f_{5/2}$ orbitals are critical to understanding the experimental β-decay properties. From the GXPF1 interaction [18], the appearance of an $N = 34$ shell gap for the Ti and Ca isotopes is based on a considerable monopole shift in the $\nu f_{5/2}$ orbital, relative to the $\nu p_{1/2}$ and $\nu p_{3/2}$ orbitals. For ^{55}Ti$_{33}$, a $1/2^-$ ground state results from the shell model calculations using GXPF1, where the effective single-particle energy for the $\nu f_{5/2}$ orbital has risen above that for $\nu p_{1/2}$. Allowed decay from a $1/2^-$ parent will selectively populate levels with $J^\pi = 1/2^-, 3/2^-$. The shell model results for ^{55}V predict only four levels having $J^\pi = 1/2^-, 3/2^-$ below 2 MeV, and nearly 70% of the calculated β decay proceeds directly to these levels. The experimental β branching is distributed between six levels below 2 MeV. Due to the high-energy Q value for the decay of ^{55}Ti, the reported β-decay branching ratios should be considered upper limits, as unobserved higher-energy γ-ray transitions may result in a shift of β strength to higher-energy levels in ^{55}V. However, the spread in the experimentally observed β branching ratios, along with the direct feeding to the ground state of ^{55}V, suggests a spin value greater than 1/2 for the ground state of ^{55}Ti. The ground state spin and parity of ^{55}V is suggested to be $7/2^-$ based on systematics, but experimentally it has been limited only to values of $3/2^-, 5/2^-$, or $7/2^-$ based on the observables for the β decay of ^{55}V [16]. A $7/2^-$ spin and parity for the ground state of ^{55}V would rule out both spin 1/2 and 3/2 for the ground state of ^{55}Ti, based on the direct β feeding of the ^{55}V ground state observed experimentally.

Since the shell model calculations using the GXPF1 interaction predict a significant gap in effective single-particle energies between the $\nu p_{1/2}$ and $\nu f_{5/2}$ orbitals for the Ti isotopes, the calculated $1/2^-$ ground state of ^{55}Ti has a dominant $\nu p_{1/2}$ component. Inspection of the ground state configurations of the $N = 33$ isotones can provide qualitative insight on the extent of the monopole shift of the $\nu f_{5/2}$ orbital with the removal of protons from the $\pi f_{7/2}$ single-particle state. The ground state spin and parity of ^{56}V$_{33}$ is 1^+ [2, 7], which can be attributed to a $\pi f^3_{7/2} \nu f^1_{5/2}$ configuration. This suggests that the $\nu f_{5/2}$ orbital, while well separated from the $\nu p_{3/2}$ orbital that results in the appearance of an $N = 32$ subshell gap, has not crossed the $\nu p_{1/2}$ orbital. The ground state spin and parity of $^{54}Sc_{33}$, which has two fewer protons in the $f_{7/2}$ orbital, is most likely 3^+ [3]. The change in ground state spin may mark the crossing of the $\nu p_{1/2}$ and $\nu f_{5/2}$ single-particle orbitals. Although effects of a significant energy gap in the effective single-particle energies for the $\nu p_{1/2}$ and $\nu f_{5/2}$ orbitals are already expected in the Ti isotopes based on the shell model results using the GXPF1 interaction, it appears from the β-decay results that the ground state of ^{55}Ti is not dominated by a simple one-neutron configuration involving either the $2p_{1/2}$ or $1f_{5/2}$ single-particle neutron orbitals.

The β-decay properties of the even-even nuclide ^{56}Ti were calculated in the same manner as ^{55}Ti. Since the ground state of ^{56}Ti is 0^+, allowed β decay will populate mainly 1^+ states in the ^{56}V daughter. The calculated spectrum of 1^+ states in ^{56}V is dense, but significant β branching is predicted to only a few states. The calculated β-branching ratios for both ^{54,56}Ti are listed in Table IV. The largest β branch in the ^{56}Ti decay, with relative intensity 81%, is to the lowest-energy 1^+ state in ^{56}V. The shell model results predict a 3^+ ground state for ^{56}V, with the first-excited state at only 160-keV excitation energy. In contrast, the ground state spin and parity of ^{56}V is 1^+ [2, 7], and the major portion of the β decay observed experimentally directly populates the 1^+ ground state. The experimental $\log ft$ value of 3.95 ± 0.12 to the ground state is well reproduced by the shell model results. Evidence for a small ($< 6\%$) β-delayed neutron branch has been found experimentally, but the shell model results show that 99.9% of the β decay Gamow-Teller strength populates 1^+ states below the one-neutron separation energy.

SUMMARY

The β decay of the neutron-rich nuclides ^{55,56}Ti has been studied, and a summary of the β-decay properties of ^{54,55,56}Ti is given in Table V. A half-life of 1.3 ± 0.1 s has been determined for ^{55}Ti, which differs significantly from previous measurements. A sharp transition in half-lives across $N = 32$, observed for many of the $\pi f_{7/2}$ neutron-rich nuclides, is not observed in Ti isotopes. The β-decay properties of ^{55}Ti, when compared to full pf-shell model calculations using the GXPF1 interaction, suggest that the ground state of ^{55}Ti is dominated by neither a $\nu p_{1/2}$ nor a $\nu f_{5/2}$ single-neutron configuration. The Ti isotopes are still in a transition region where the monopole shift in the $\nu f_{5/2}$ orbital due to the removal of protons from the $\pi f_{7/2}$ orbital has not yet produced complete separation of pf-shell orbitals. This separation, as predicted by the shell model calculations using the GXPF1 interaction, may not fully develop until the Ca isotopes.

This work was supported in part by the National Science Foundation Grants PHY-01-10253, PHY-97-24299, and PHY-02-44453. The authors would like to thank the NSCL operations staff for providing the primary and secondary beams for this experiment.

---

[1] J.I. Prisciandaro, P.F. Mantica, B.A. Brown, D.W. Anthony, M.W. Cooper, A. Garcia, D.E. Groh, A. Komives, W. Kumarasiri, P.A. Lofy, A.M. Oros-Peusquens, S.L. Tabor, and W. Wiedeking, Phys. Lett. B**510**, 17 (2001).

[2] P.F. Mantica, A.C. Morton, B.A. Brown, A.D. Davies, T. Glasmacher, D.E. Groh, S.N. Liddick, D.J. Morrissey, W.F. Mueller, H. Schatz, A. Stolz, S.L. Tabor, M. Honma, M. Horoi, and T. Otsuka, Phys. Rev. C **67**, 014311 (2003).

[3] R.V.F. Janssens, B. Fornal, P.F. Mantica, B.A. Brown, R. Broda, P. Bhattacharyya, M.P. Carpenter, M. Cinausero, P.J. Daly, A.D. Davies, T. Glasmacher, Z.W. Grabowski, D.E. Groh, M. Honma, F.G. Kondev, W. Krolas, T. Lauritsen, S.N. Liddick, S. Lunardi, N. Marginean, T. Mizusaki, D.J. Morrissey, A.C. Morton, W.F. Mueller, T. Otsuka, T. Pawlat, D. Seweryniak, H. Schatz, A. Stolz, S.L. Tabor, C.A. Ur, G. Viesti, I. Wiedenhoever, and J. Wrzesinski, Phys. Lett. B**546**, 55 (2002).

[4] D.E. Appelbe, C.J. Barton, M.H. Muikku, J. Simpson, D.D. Warner, C.W. Beausang, M.A. Caprio, J.R. Cooper, J.R. Novak, N.V. Zamfir, R.A.E. Austin, J.A. Cameron, C. Malcolmson, J.C. Waddington, and R.F. Xu, Phys. Rev. C **67**, 034309 (2003).

[5] T. Otsuka, R. Fujimoto, Y. Utsuno, B.A. Brown, M. Honma, and T. Mizusaki, Phys. Rev. Lett. **87**, 082502 (2001).

[6] S.Y.F. Chu, L.P. Ekström, and R.B. Firestone, WWW Table of Radioactive Isotopes, database version 1999-02-28 from URL http://nucleardata.nuclear.lu.se/nucleardata/toi/.

[7] O. Sorlin, V. Borrel, S. Grévy, D. Guillemaud-Mueller, A.C. Mueller, F. Pougheon, W. Böhmer, K.-L. Kratz, T. Mehren, P. Möller, B. Pfeiffer, T. Rauscher, M.G. Saint-Laurent, R. Anne, M. Lewitowicz, A. Ostrowski, T. Dörfler, and W.D. Schmidtt-Ott, Nucl. Phys. **A632**, 205 (1998).

[8] T. Dörfler, W.-D. Schmidt-Ott, T. Hild, T. Mehren, W. Böhmer, P. Möller, B. Pfeiffer, T. Rauscher, K.-L. Kratz, O. Sorlin, V. Borrel, S. Grévy, D. Guillemaud-Mueller, A.C. Mueller, F. Pougheon, R. Anne, M. Lewitowicz, A. Ostrowsky, M. Robinson, and M.G. Saint-Laurent, Phys. Rev. C **54**, 2894 (1996).

[9] F. Ameil, M. Bernas, P. Armbruster, S. Czajkowski, Ph. Dessagne, H. Geissel, E. Hanelt, C. Kozhuharov, C. Miehe, C. Donzaud, A. Grewe, A. Heinz, Z. Janas, M. deJong, W. Schwab, and S. Steinhäuser, Eur. J. Phys. A **1**, 275 (1998).

[10] M. Langevin, C. Detraz, D. Guillemaud-Mueller, A.C. Mueller, C. Thilbault, F. Touchard, G. Klotz, C. Miehe, G. Walter, M. Epherre, and C. Richard-Serre, Phys. Lett. **130B**, 251 (1983).

[11] D.J. Morrissey, B.M. Sherrill, M. Steiner, A. Stolz, and I. Wiedenhöver, Nucl. Instrum. Methods Phys. Res. B **204**, 90 (2003).

[12] J.I. Prisciandaro, A.C. Morton, and P.F. Mantica, Nucl. Instrum. Methods Phys. Res. A **505**, 140 (2003).

[13] W.F. Mueller, J.A. Church, T. Glasmacher, D. Gutknecht, G. Hackman, P.G. Hansen, Z. Hu, K.L. Miller, P. Quirin, Nucl. Instrum. Methods Phys. Res. A **466**, 492 (2001).

[14] G. Audi and A.H. Wapstra, Nucl. Phys. **A595**, 409 (1995).

[15] N.B. Gove and M.J. Martin, At. Data Nucl. Data Tables **10**, 206 (1971).

[16] A.M. Nathan, D.E. Alburger, J.W. Olness, and E.K. Warburton, Phys. Rev. C **16**, 1566 (1977).

[17] T.W. Burrows, Nucl. Data Sheets **76**, 191 (1995).

[18] M. Honma, T. Otsuka, B.A. Brown, and T. Mizusaki, Phys. Rev. C **65**, 061301R (2002).

[19] B.A. Brown, A. Etchegoyen and W.D.M. Rae, The computer code OXBASH, MSU-NSCL report number 524 (1998).

[20] M. Horoi, B.A. Brown, and V. Zelevinsky, Phys. Rev. C **67**, 034303 (2003).

[21] A. Poves, J. Sanchez-Solano, E. Caurier, and F. Nowacki, Nucl. Phys. **A694**, 157 (2001).

FIG. 1: β-delayed γ-ray spectrum for ^{55}Ti in the range 0 to 2 MeV. This spectrum includes events within the first second after a ^{55}Ti implant. The peaks labeled by energy have been assigned as transitions following the decay of ^{55}Ti unless otherwise noted.

FIG. 2: Decay curves for ^{55}Ti, showing (a) fragment-β correlations only, where the data were fitted with a single exponential decay with exponential background; (b) fragment-β correlations with an additional requirement of a 323-keV γ ray; and (c) fragment-β correlations with an additional requirement of a 673-keV γ ray. The curves shown in (b) and (c) were fitted with a single exponential with constant background.

FIG. 3: Proposed level scheme for ^{55}V populated following the β decay of ^{55}Ti. The number in brackets following the γ-ray decay energy is the absolute γ intensity in percent. The Q_β value was deduced from data in Ref. [14]. Identified coincidence relationships are shown by the filled circles.

FIG. 4: γ rays in coincidence with the (a) 323-keV, (b) 673-keV, and (c) 828-keV γ-ray transitions following ^{55}Ti β decay.

FIG. 5: (a) Decay curve for ^{56}Ti. Data were fitted with a single exponential decay and exponential growth and decay of the short-lived daughter ^{56}V. An exponential background is also considered in the fit. (b) β-delayed γ-ray spectrum for ^{56}Ti in the range 0 to 1.5 MeV. A gate was placed on the decay curve to include only events within the first second of a ^{56}Ti implant. The 668- and 1006-keV γ rays from decay of the daughter ^{56}V dominate the spectrum. One inset shows an expanded view of the γ-ray spectrum in the region around 160 keV. The 13 counts in a single channel at 162 keV are proposed to be a spectrum artifact. For comparison, an expansion of the region around 1006 keV is shown in a second inset.

FIG. 6: Shell model results for the β decay of ^{55}Ti. Details of the shell model calculations are given in the text. The ^{55}V experimental levels and β decay branching ratios derived in the present work are shown to the right.

TABLE I: Experimental half-lives for neutron-rich nuclides with $N = 32$ and $N = 33$. Half-lives are taken from Ref. [6] unless noted otherwise. Decay of the neutron-rich K isotopes, with a hole in the proton *sd* shell, will result in production of Ca daughters that have a filled proton *sd* shell in the ground state, while decay of the other parents listed will produce daughter nuclides having a partially-filled proton $f_{7/2}$ orbital.

	$T_{1/2}$ (s)		
Element	$N = 32$	$N = 33$	$T_{1/2}^{N=32}/T_{1/2}^{N=33}$
$_{19}$K	0.365	0.105	3.5
$_{20}$Ca	4.6	0.090	51
$_{21}$Sc	$> 3^a$	0.225^a	> 13
$_{22}$Ti	1.5^b	0.60^b, 0.32^c	2.5^b, 5.0^c
$_{23}$V	6.54	0.216^d	30
$_{24}$Cr	356	21.1	16
$_{25}$Mn	85.4	3.0	28

[a] Ref. [7].
[b] Ref. [8].
[c] Ref. [9].
[d] Ref. [2].

TABLE II: γ rays observed following the decay of ^{55}Ti.

E_γ(keV)	I_γ^{abs}(%)	Initial State (keV)	Final State (keV)
323.4 ± 0.4	20 ± 2	323	0
349.3 ± 0.6	3 ± 1	673	323
651.6 ± 0.7	5 ± 1	2153	1501
672.5 ± 0.4	44 ± 4	673	0
828.1 ± 0.5	10 ± 2	1501	673
1262.5 ± 0.6	5 ± 1		
1330.1 ± 0.5	12 ± 2	1330	0
1480.0 ± 0.8	6 ± 1	2153	673
1830.0 ± 0.8	5 ± 1	2153	323

TABLE III: β intensities and log*ft* values for the ^{55}Ti decay to bound levels in ^{55}V.

E(keV)	I_β(%)	log(*ft*)[a]
0	24 ± 5	5.41 ± 0.23
323.4 ± 0.4	12 ± 3	5.61 ± 0.28
672.6 ± 0.4	31 ± 5	5.20 ± 0.20
1330.1 ± 0.5	12 ± 2	5.31 ± 0.20
1500.7 ± 0.7	5 ± 3	5.63 ± 0.61
2152.8 ± 0.6	16 ± 2	4.87 ± 0.20

[a]Based on $Q_\beta = 7.3 \pm 0.3$ MeV [14] and $T_{1/2} = 1.3 \pm 0.1$ s.

TABLE IV: Calculated β-decay branching ratios for the ground-state decay of even-even ^{54,56}Ti to calculated 1^+ states in the daughter ^{54,56}V nuclides. Details regarding the shell model calculations using the GXPF1 interaction are given in the text.

^{54}Ti $\rightarrow$ ^{54}V			^{56}Ti $\rightarrow$ ^{56}V		
E(keV)	I_β(%)	log(*ft*)	E(keV)	I_β(%)	log(*ft*)
460	0.4	6.61	160	81.4	3.87
729	64.3	4.26	933	2.7	5.10
1562	27.7	4.12	1215	0.1	7.04
1936	4.6	4.63	1761	8.8	4.31
2108	0.1	6.10	1901	2.3	4.84
2361	0.3	5.40	2212	0.2	5.88
Sum	97.4		Sum	95.5	

TABLE V: Summary of the β-decay properties derived in this work compared to shell model results using the GXPF1 interaction.

			$T_{1/2}$(s)				Ground state β branch (%)		
Isotope	$J^{\pi}_{\text{g.s.}}$	Q_β (MeV)[a]	Theory[b]	Expt.	Ref. [9]	Ref. [8]	Theory	Expt.	Ref. [7]
^{54}Ti	0^+	4.28 ± 0.16	12 ± 3			1.5 ± 0.4	0.4		< 10
^{55}Ti	$1/2^-$	7.3 ± 0.3	2.5 ± 0.5	1.3 ± 0.1	0.32 ± 0.06	0.60 ± 0.04	0	24 ± 5	60 ± 10
^{56}Ti	0^+	7.1 ± 0.4	0.33 ± 0.09	0.200 ± 0.005	0.19 ± 0.04	0.15 ± 0.03	81	94 ± 3	~ 60

[a]Taken from Ref. [14].

[b]The calculated half-lives were multiplied by a factor of 2 to account for the known reduction in calculated Gamow-Teller strength in the full space when compared to experiment [21]. The error in the theoretical half-life comes from the error in the reported Q value.

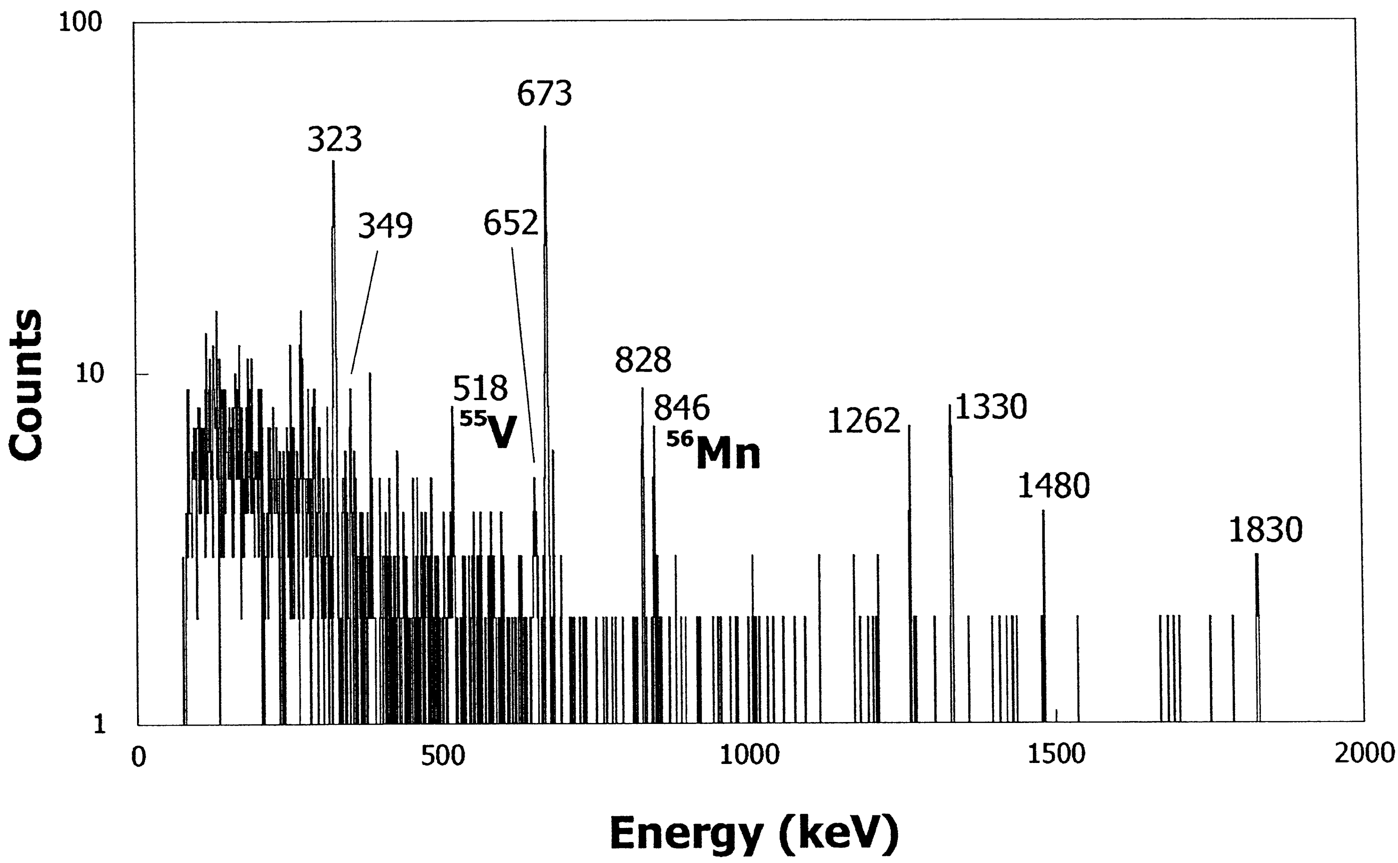

100
10
1
Counts
323
349
673
652
518
55V
828
846
56Mn
1262
1330
1480
1830
0
500
1000
1500
2000
Energy (keV)

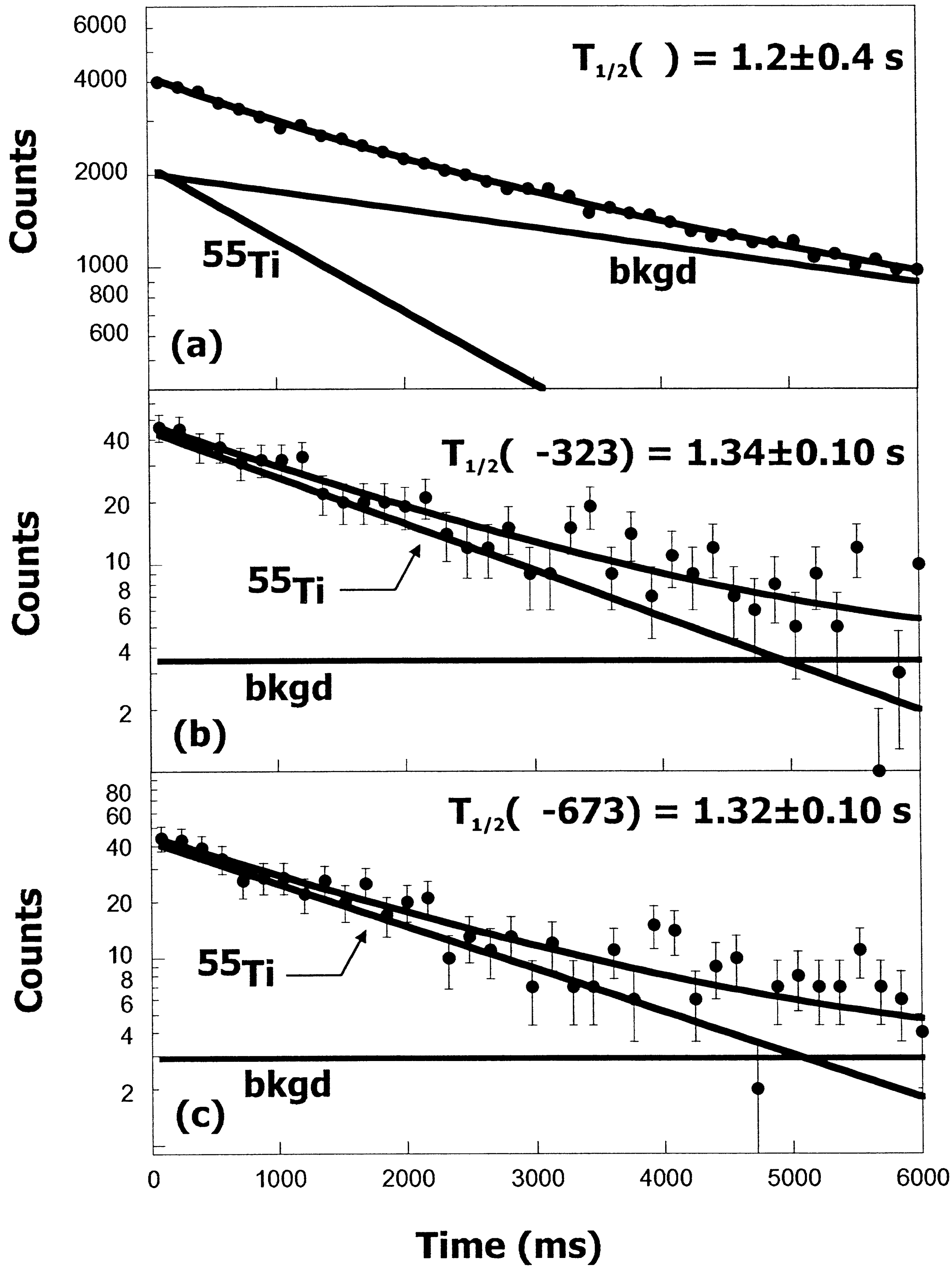

T1/2( ) = 1.2±0.4 s
55Ti
bkgd
(a)
T1/2(-323) = 1.34±0.10 s
55Ti
bkgd
(b)
T1/2(-673) = 1.32±0.10 s
55Ti
bkgd
(c)
Counts
Time (ms)

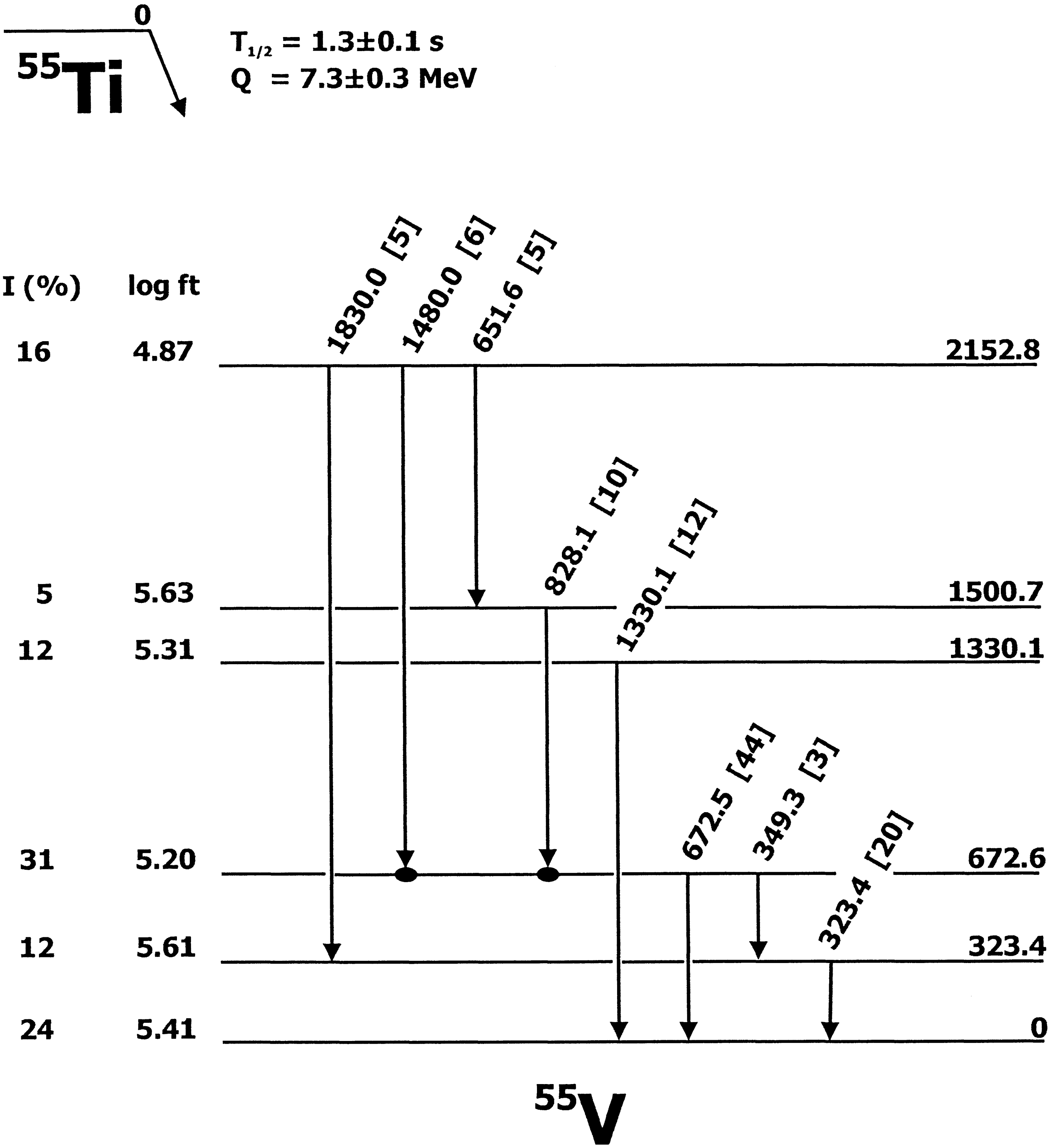
0
55Ti
T1/2 = 1.3±0.1 s
Q = 7.3±0.3 MeV
I (%)
log ft
16
4.87
1830.0 [5]
1480.0 [6]
651.6 [5]
2152.8
828.1 [10]
1330.1 [12]
5
5.63
1500.7
12
5.31
1330.1
672.5 [44]
349.3 [3]
323.4 [20]
31
5.20
672.6
12
5.61
323.4
24
5.41
0
55V

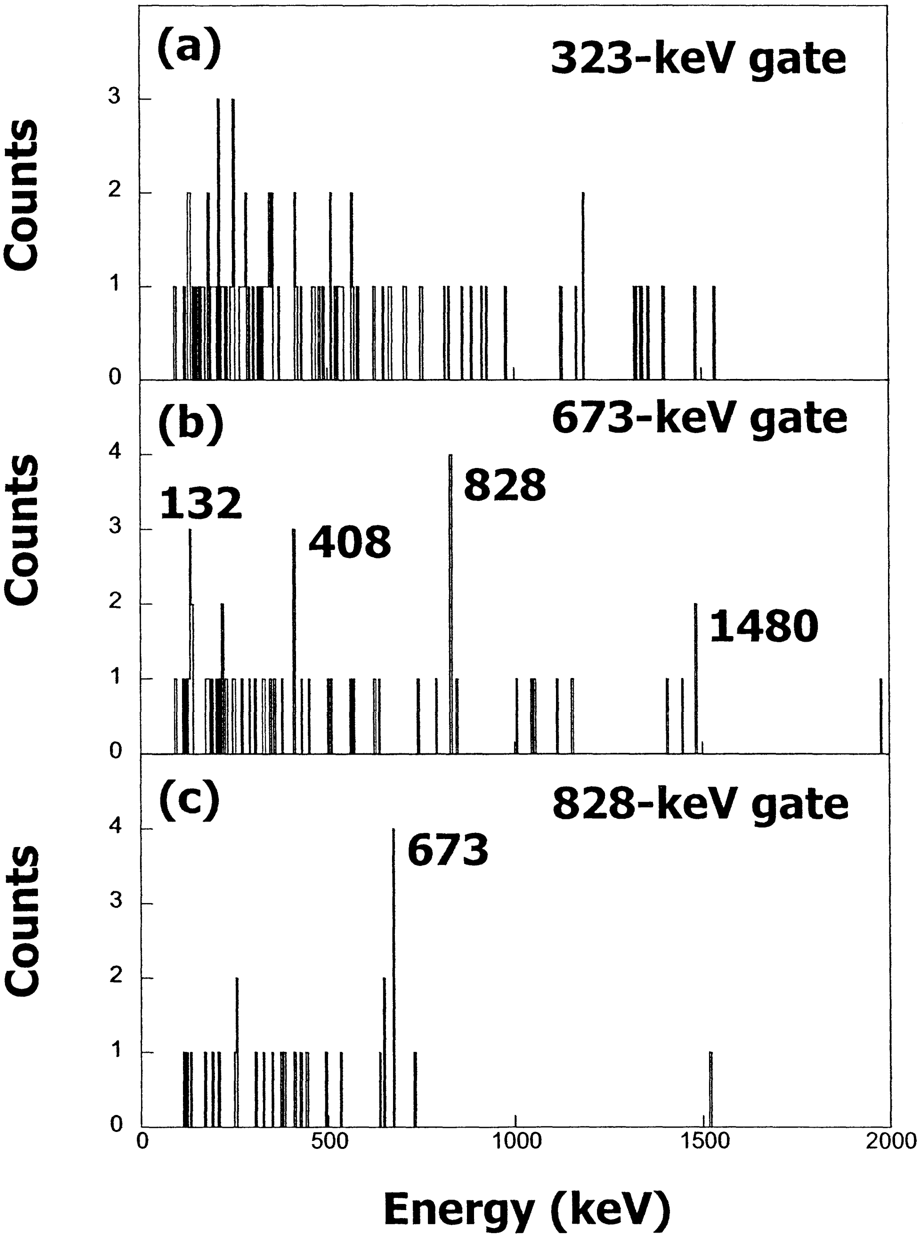

(a)
323-keV gate
(b)
673-keV gate
132
408
828
1480
(c)
828-keV gate
673
Counts
Counts
Counts
0
1
2
3
0
1
2
3
4
0
1
2
3
4
0
500
1000
1500
2000
Energy (keV)

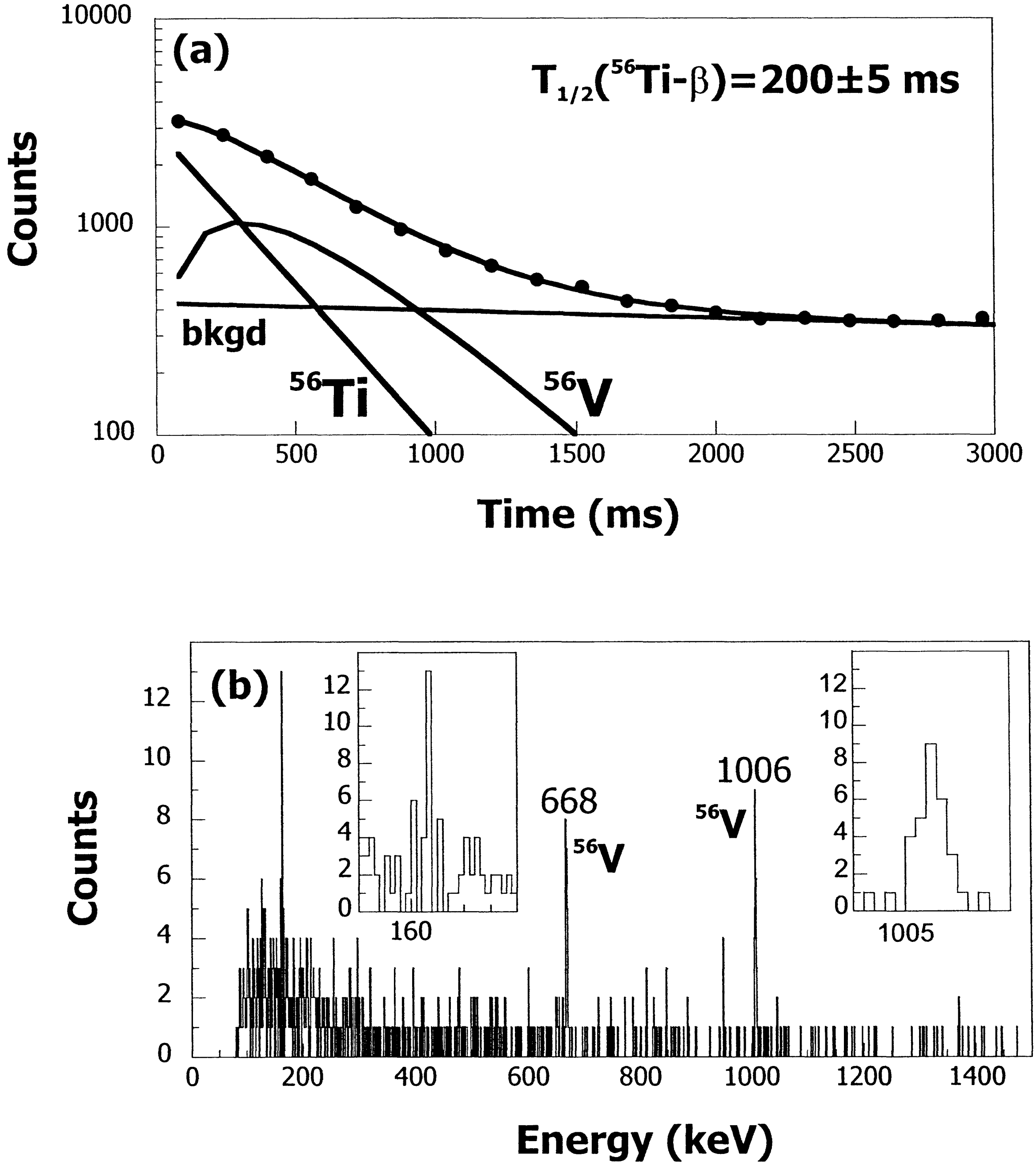

(a)
T1/2(56Ti-β)=200±5 ms
Counts
10000
1000
100
bkgd
56Ti
56V
0
500
1000
1500
2000
2500
3000
Time (ms)
(b)
Counts
0
2
4
6
8
10
12
160
1005
668
56V
1006
56V
0
200
400
600
800
1000
1200
1400
Energy (keV)

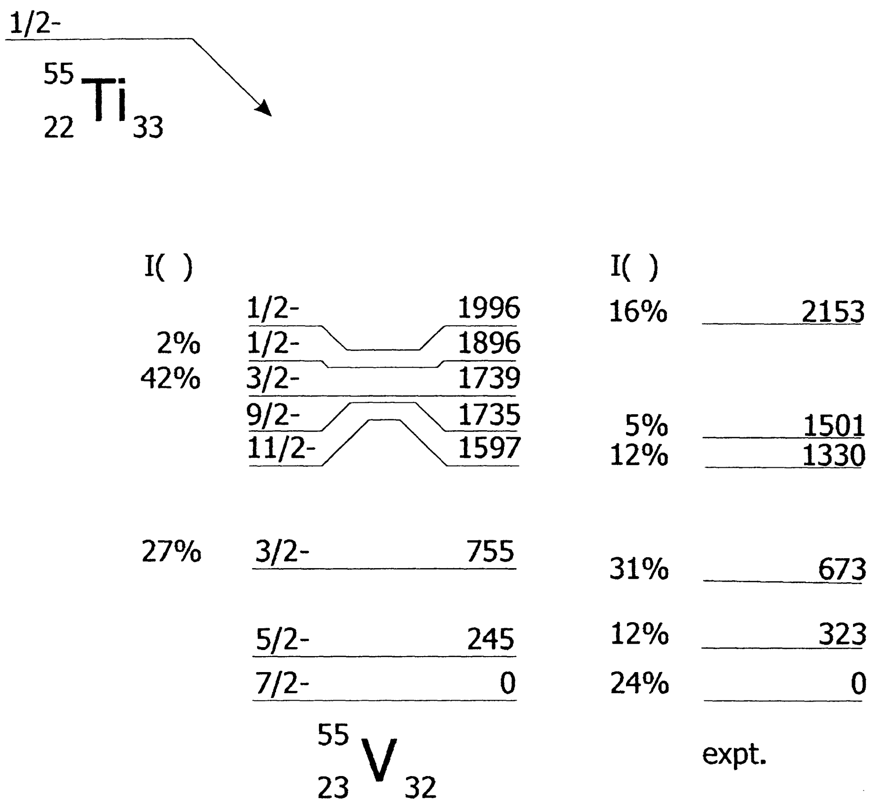
1/2-
55 Ti 22 33
I( )
1/2- 1996
2% 1/2- 1896
42% 3/2- 1739
9/2- 1735
11/2- 1597
27% 3/2- 755
5/2- 245
7/2- 0
55 V 23 32
I( )
16% 2153
5% 1501
12% 1330
31% 673
12% 323
24% 0
expt.